

Model-Potential Calculation of the Density of States in Liquid and Solid Lithium, Cadmium, and Indium*

ROBERT W. SHAW, JR.†

Division of Applied Physics, Stanford University, Stanford, California 94305

AND

NEVILLE V. SMITH

Stanford Electronics Laboratory, Stanford University, Stanford, California 94305

(Received 15 July 1968)

A perturbation expansion of the electron energy has been used to calculate the density of states in liquid lithium, cadmium, and indium. The full nonlocal form of the optimum model potential proposed by Shaw has been used in these calculations. It is shown by comparing the nonlocal calculation to various approximate calculations that the nonlocal effects produce large changes in the second-order corrections to the electron energy and a considerable smoothing of the structure in the density of states. The first-order, k -dependent corrections to the electron energy have been included, and k -dependent effective masses have been calculated for several elements. The density of states for crystalline lithium, cadmium, and indium has also been calculated by determining the distortion of energy surfaces due to the first few zone planes. The results for liquid and solid are compared, and agreement with experiment is discussed.

I. INTRODUCTION

CONSIDERABLE effort has been devoted to the study of liquid metals in recent years.¹⁻⁵ Most of this work has been concerned with developing formal methods; few attempts have been made to evaluate the theoretical expressions numerically and compare the results with experiment. Ballentine⁵ has calculated the density of states for several liquid metals using results from the Green's-function theory due to Edwards.² However, Ballentine used a local, energy-independent form of the Heine-Abarenkov model potential in his calculations. In attempting to use Ballentine's method for other metals, we found that the results were extremely sensitive to the position of the first form-factor node. This was a disturbing observation because it is well known^{6,7} that the form factor is not uniquely defined, and that the precise position of the node can, therefore, have no physical significance. Since there is no *a priori* reason to suspect that perturbation theory cannot be used to compute the density of states, we considered the validity of using a local form factor. Recent work on the model potential^{8,9} has shown that nonlocal effects can be appreciable. We have, therefore, used the full nonlocal form of the optimum model potential⁹ to calculate the electronic energy and the

density of states for liquid lithium, cadmium, and indium. We find that structure in these properties is reduced relative to the results of similar local calculations and that the results are insensitive to arbitrary changes in the potential.

Our motivation for considering lithium, cadmium, and indium was primarily experimental. Recent photoemission experiments on indium in the solid and liquid states^{10,11} have shown that the energy distributions of photoemitted electrons exhibit pronounced structure which has been tentatively attributed¹⁰ to structure in the density of filled states. Part of the structure is found to disappear in the liquid state, suggesting a large change in the density of states on melting. Our aim was to provide a theoretical test of this interpretation. It will be seen below that our theoretical results throw doubt on the adequacy of this explanation of the photoemission data. Cadmium differs from most other metals in that it shows a large jump in the Knight shift at the melting point.¹² Ziman¹³ has attributed this to an abrupt change in the Fermi-surface density of states, but no detailed theoretical calculation has been done. Lithium is of particular interest since Ham¹⁴ has predicted rather large deviations from the free-electron density of states in the solid. We wished to determine if these deviations persist into the liquid. In addition, the three metals provide examples of monovalent, divalent, and trivalent behavior.

In each of the three metals there is, therefore, some reason to suppose that the density of states might change quite appreciably on melting. In order to test this possibility, we need calculations of the solid density

* Work supported by the Advanced Research Project Agency through the Center for Materials Research at Stanford University.

† Present address: Cavendish Laboratory, Cambridge, England.

¹ P. Phariseau and J. M. Ziman, *Phil. Mag.* **8**, 1487 (1963).

² S. F. Edwards, *Phil. Mag.* **6**, 617 (1961); *Proc. Roy. Soc. (London)* **A267**, 518 (1962).

³ L. E. Ballentine and V. Heine, *Phil. Mag.* **9**, 617 (1964).

⁴ T. E. Faber, *Advan. Phys.* **15**, 547 (1966).

⁵ L. E. Ballentine, *Can. J. Phys.* **44**, 2533 (1966).

⁶ B. J. Austin, V. Heine, and L. J. Sham, *Phys. Rev.* **127**, 276 (1962).

⁷ W. A. Harrison, *Pseudopotentials in the Theory of Metals* (W. A. Benjamin, Inc., New York, 1966).

⁸ R. W. Shaw, Jr., and W. A. Harrison, *Phys. Rev.* **163**, 604 (1967).

⁹ R. W. Shaw, Jr., *Phys. Rev.* **174**, 769 (1968).

¹⁰ R. Koyama, W. E. Spicer, N. W. Ashcroft, and W. E. Lawrence, *Phys. Rev. Letters* **19**, 1284 (1967).

¹¹ R. Koyama and W. E. Spicer (unpublished).

¹² E. F. W. Seymour and G. A. Styles, *Phys. Letters* **10**, 269 (1964).

¹³ J. M. Ziman, *Advan. Phys.* **16**, 421 (1967).

¹⁴ F. S. Ham, *Phys. Rev.* **128**, 2524 (1962).

of states with which to compare. It is clear that such a comparison will be most meaningful if the solid and liquid calculations have been performed with the same potential and by essentially the same method. This consideration led us to make calculations of the solid density of states. The method consists of determining the distortion of the constant energy surfaces due to the presence of the first three zone planes.

The paper is divided into four parts: We discuss, first, the perturbation approach, which we have used to calculate the density of states in liquid metals. Then we consider in some detail the evaluation of first- and second-order corrections to the electron energy and the corresponding density-of-states corrections. In Sec. IV, we discuss the method for computing density of states in crystalline metals and compare the results with those obtained for the liquid. Finally, we compare our calculations to experimental results.

II. ELECTRONIC STRUCTURE OF LIQUID METALS

A. Perturbation Theory

To a very good approximation, liquid metals can be studied using standard perturbation techniques. The calculations proceed exactly as for crystalline simple metals.^{7,15} We replace the crystal potential with a weak model or pseudopotential, W , which may be written as the sum of potentials at individual ion sites:

$$W = \sum_i w_i. \quad (2.1)$$

The Schrödinger equation for the metal is now replaced by a model wave equation,

$$(T+W)|\chi_k\rangle = E_k|\chi_k\rangle, \quad (2.2)$$

where $|\chi_k\rangle$ is a smooth model (or pseudo-) wave function. The unperturbed model wave functions are plane waves. Therefore, the perturbation expansion for $|\chi_k\rangle$ is simply

$$|\chi_k\rangle = [1 + a_0(k)]|\mathbf{k}\rangle + \sum_{\mathbf{q}}' a_{\mathbf{q}}(k)|\mathbf{k}+\mathbf{q}\rangle. \quad (2.3)$$

We regard the coefficients $a_{\mathbf{q}}(\mathbf{k})$ as first-order quantities, substitute (2.3) into the model wave equation, and calculate $a_{\mathbf{q}}(k)$ and E_k , using ordinary perturbation theory. The result for E_k is simply (we use atomic units throughout)

$$E_k = \frac{1}{2}k^2 + N\langle\mathbf{k}|w|\mathbf{k}\rangle + \sum_{\mathbf{q}}' |S(\mathbf{q})|^2 \frac{N^2\langle\mathbf{k}|w|\mathbf{k}+\mathbf{q}\rangle\langle\mathbf{k}+\mathbf{q}|w|\mathbf{k}\rangle}{\frac{1}{2}(k^2 - |\mathbf{k}+\mathbf{q}|^2)}. \quad (2.4)$$

In this expression the off-diagonal matrix elements of the single-ion model potential, $\langle\mathbf{k}+\mathbf{q}|w|\mathbf{k}\rangle$, which are

¹⁵ W. A. Harrison, *Advan. Phys.* **16**, 383 (1967).

referred to as form factors, are, in general,^{8,9} functions of the magnitude of \mathbf{k} and \mathbf{q} and of the angle between them.

The structure factor, $S(\mathbf{q})$, is zero except at reciprocal-lattice vectors for a perfect crystalline solid. However, for a liquid, $S(\mathbf{q})$ is nonzero for all wave vectors. It is customary to define a liquid interference function, $a(q)$, as follows:

$$a(q) = N|S(\mathbf{q})|^2 = \frac{1}{N} \sum_i \sum_j e^{i(\mathbf{x}_i - \mathbf{x}_j) \cdot \mathbf{q}}. \quad (2.5)$$

This interference function is obtainable from x-ray and neutron-scattering measurements on liquids. One can also attempt a direct calculation of $a(q)$, using, for example, the Percus-Yevick theory as done by Ashcroft and Lekner.¹⁶ We will not be concerned with the calculation of $a(q)$ but will use either x-ray data or Ashcroft-Lekner functions in our calculations.

Since $a(q)$ is a continuous function of q , we must convert the sum to an integral using the relation

$$\sum_{\mathbf{q}}' \rightarrow \frac{\Omega}{(2\pi)^3} P \int d^3q. \quad (2.6)$$

Note that there is no spin degeneracy to be accounted for in this conversion. For a liquid metal, the perturbation expansion for the electron energy may then be written

$$E_k = \frac{1}{2}k^2 + N\langle\mathbf{k}|w|\mathbf{k}\rangle - \frac{2\Omega_0}{(2\pi)^3} \int d^3q \frac{a(q)|w_{\mathbf{q}}(\mathbf{k})|^2}{q^2 + 2\mathbf{k} \cdot \mathbf{q}}, \quad (2.7)$$

where

$$\Omega_0 = \text{atomic volume} = \Omega/N, \quad w_{\mathbf{q}}(\mathbf{k}) = N\langle\mathbf{k}+\mathbf{q}|w|\mathbf{k}\rangle.$$

The perturbation expansion for E_k in a solid is singular when \mathbf{k} falls on a zone plane. To obtain the dispersion in the region of zone planes, we must diagonalize a degenerate matrix (Sec. IV). In a liquid there is a singularity for every \mathbf{k} since we are integrating over q instead of summing over reciprocal-lattice vectors. The prescription for handling this singularity is, in the spirit of nondegenerate perturbation theory, to conduct the integral in (2.7) as a principal-value integral.⁷

The density of states may be obtained from the electron energy by using the general expression

$$N(E) = \frac{2\Omega}{(2\pi)^3} \int \frac{dS_k}{|\nabla_{\mathbf{k}} E_k|}, \quad (2.8)$$

where the integration is over constant energy surfaces. For a liquid, these surfaces are isotropic, and (2.8) may be written

$$\frac{N(E)}{N_{\text{FB}}(E)} = k \left(\frac{\partial E_k}{\partial k} \right)^{-1}. \quad (2.9)$$

¹⁶ N. W. Ashcroft and J. Lekner, *Phys. Rev.* **145**, 83 (1966).

$N_{FE}(E)$ is the free-electron density of states. We will use the perturbation expression for E_k to evaluate Eq. (2.9). The important point to note here is that we will use the full nonlocal model potential to evaluate the second-order term in (2.7). We will discuss in some detail why this careful evaluation of the energy is essential after we compare our approach to the more standard Green's-function method.

B. Green's-Function Method

Perhaps the most unsatisfying feature of the simple perturbation treatment of liquid metals is that we have regarded the liquid wave functions, Eq. (2.3), as perturbations around a single plane wave with a well-defined crystal momentum \mathbf{k} . As Edwards² and Faber⁴ have pointed out, a more reasonable wave function for a metal is a packet, centered around a wave number \mathbf{k} ,

$$|\chi_k\rangle = \sum_q a_q(\mathbf{k}) |\mathbf{k}+\mathbf{q}\rangle, \quad (2.10)$$

in which the components around and including $q=0$ are all weighted about equally. That is, in (2.10) all of the $a_q(\mathbf{k})$ are of the same order, whereas in (2.3) the $q=0$ component has a zero-order weight and all the other components are of first order.

We now substitute (2.10) into the model wave equation and obtain an expression for the coefficients,

$$a_q(\mathbf{k}) = \frac{1}{E - \frac{1}{2}|\mathbf{k}+\mathbf{q}|^2} \sum_{q'} a_{q'}(\mathbf{k}) \langle \mathbf{k}+\mathbf{q} | W | \mathbf{k}+\mathbf{q}' \rangle, \quad (2.11)$$

where E is the exact energy of the state. This expression may be iterated by substituting an analogous expression for $a_{q'}(\mathbf{k})$ into the sum. At each step, we extract the term proportional to $a_q(\mathbf{k})$. Suppose for convenience we consider the $q=0$ case and proceed with the iteration. The result after two iterations is, for example,

$$\begin{aligned} (E - \frac{1}{2}k^2) a_0(\mathbf{k}) &= a_0(\mathbf{k}) \\ &\times \left\{ \langle \mathbf{k} | W | \mathbf{k} \rangle + \sum_{q \neq 0} \frac{\langle \mathbf{k} | W | \mathbf{k}+\mathbf{q} \rangle \langle \mathbf{k}+\mathbf{q} | W | \mathbf{k} \rangle}{E - \frac{1}{2}|\mathbf{k}+\mathbf{q}|^2} \right\} \\ &+ \sum_{q, q' \neq 0} a_{q'}(\mathbf{k}) \frac{\langle \mathbf{k} | W | \mathbf{k}+\mathbf{q} \rangle \langle \mathbf{k}+\mathbf{q} | W | \mathbf{k}+\mathbf{q}' \rangle}{E - \frac{1}{2}|\mathbf{k}+\mathbf{q}|^2}. \end{aligned} \quad (2.12)$$

If we continue this iteration indefinitely, the coefficient $a_0(\mathbf{k})$ cancels out, and on the right we have an infinite series of terms which includes all scattering diagrams in which no internal momentum is equal to the external momentum \mathbf{k} . This series is precisely what is referred to as the electron self-energy, $\langle \mathbf{k} | \Sigma | \mathbf{k} \rangle$. In terms of this self-energy, the dispersion is now simply

$$E - \frac{1}{2}k^2 - \langle \mathbf{k} | \Sigma | \mathbf{k} \rangle = 0. \quad (2.13)$$

This is a well-known result and is identical to the dispersion relation obtained from the poles of the one-

electron Green's function evaluated in the \mathbf{k} representation,

$$G(\mathbf{k}, E) = 1 / \{ E - \frac{1}{2}k^2 - \langle \mathbf{k} | \Sigma | \mathbf{k} \rangle \}, \quad (2.14)$$

as discussed by Edwards² and Ballentine.⁵

It is interesting to note that we could have obtained a result analogous to (2.13) by iterating (2.11) for arbitrary q ,

$$E - \frac{1}{2}|\mathbf{k}+\mathbf{q}|^2 - \langle \mathbf{k}+\mathbf{q} | \Sigma | \mathbf{k}+\mathbf{q} \rangle = 0. \quad (2.15)$$

This does not mean that E is not uniquely defined, provided we evaluate the self-energy to all orders. One obtains the same result in Green's-function theory if one takes the $|\mathbf{k}+\mathbf{q}\rangle$ diagonal matrix element of the Green's function

$$\begin{aligned} G(E) &= (E - H_0 - V)^{-1} = G_0 + G_0 V G_0 + G_0 V G_0 V G_0 + \dots, \\ G_0 &= (E - H_0)^{-1}, \end{aligned} \quad (2.16)$$

instead of the $|\mathbf{k}\rangle$ diagonal element. However, it does mean that the first few terms of a perturbation expansion will not necessarily yield the same result. This is simply a reflection of the fact that in writing (2.10), we have acknowledged that crystal momentum is not a well-defined quantum number in a liquid. We cannot, therefore, expect E to be a uniquely defined function of momentum. It has, however, become customary to describe the state in terms of the momentum \mathbf{k} at the wave packet center, as we have indicated in (2.10) by labeling the state with \mathbf{k} . We will adopt this convention and use (2.13) to compute the energy.

If we expand (2.13) to second order in W we obtain

$$E = \frac{1}{2}k^2 + N \langle \mathbf{k} | w | \mathbf{k} \rangle + \sum_{q \neq 0} \frac{|S(\mathbf{q})|^2 |w_q(\mathbf{k})|^2}{E - \frac{1}{2}|\mathbf{k}+\mathbf{q}|^2}. \quad (2.17)$$

The perturbation approximation we made previously was to replace E in (2.17) by its zero-order value $\frac{1}{2}k^2$. This is a consistent procedure within the framework of ordinary perturbation theory in which matrix elements of W are regarded as first-order quantities. We recall that exactly the same approximation has been made in the self-consistent screening of the model potential. Therefore, to justify a more elaborate approximation in the energy calculation, one ought to redo the screening in the same framework.

Though we are inclined to view the simple perturbation approach as the most justifiable method for computing the energy of electron states in a liquid, this point of view is not presently in vogue. We will, therefore, consider an alternative scheme due to Ballentine⁶ and investigate numerically the difference between the two approaches. Ballentine has attempted to introduce a certain internal consistency by arbitrarily replacing the zero-order propagator in the second-order self-energy by the exact propagator, $G(k, E)$,

$$\langle \mathbf{k} | \Sigma_2 | \mathbf{k} \rangle = \sum_{q \neq 0} \frac{|S(\mathbf{q})|^2 |w_q(\mathbf{k})|^2}{E - \frac{1}{2}|\mathbf{k}+\mathbf{q}|^2 - \langle \mathbf{k}+\mathbf{q} | \Sigma | \mathbf{k}+\mathbf{q} \rangle}. \quad (2.18)$$

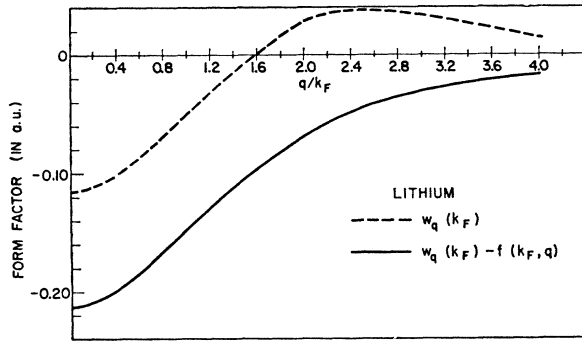


FIG. 1. Optimized model-potential form factor for lithium (dashed line) and the \mathbf{k} -independent part of the form factor (solid line).

This approximation is equivalent to extracting a particular set of diagrams from the self-energy expression and summing these diagrams exactly to all orders in the perturbation W . This has the effect of introducing a lifetime broadening of the wave packet, if Σ has an imaginary part. Also, Ballentine found that in order to evaluate (2.18) it was necessary to suppress the q dependence of $\langle \mathbf{k} + \mathbf{q} | \Sigma | \mathbf{k} + \mathbf{q} \rangle$ in the energy denominator. If we make the same approximation and use Eq. (2.13), we immediately obtain Eq. (2.4). Ballentine's approach, therefore, differs from ours only in that we have not included an imaginary part of the self-energy. This is reasonable since it is clear from (2.12) that the self-energy obtained by perturbation theory is explicitly real. In addition, it is not entirely self-consistent to include lifetime broadening in the energy calculation since it has not been included in the screening of the potential. We have, however, investigated numerically the importance of lifetime broadening (Sec. III).

The expression we have given for the density of states, Eq. (2.9), is equivalent to the usual result obtained from Green's-function theory when the imaginary part of the self-energy is zero, which is the case if (2.7) is to be used.¹⁷ The density of states is defined as an integral over a spectral density, $\rho(\mathbf{k}, E)$:

$$N(E) = \frac{2\Omega}{(2\pi)^3} \int d^3k \rho(\mathbf{k}, E). \quad (2.19)$$

The spectral density is related to the Green's function by

$$\rho(\mathbf{k}, E) = (-1/\pi) \text{Im} G(\mathbf{k}, E + i\epsilon) \\ = \delta(E - \frac{1}{2}k^2 - \langle \mathbf{k} | \Sigma | \mathbf{k} \rangle), \quad (2.20)$$

where in writing the δ function we have used the fact that the $\langle \mathbf{k} | \Sigma | \mathbf{k} \rangle$ is real. If we substitute (2.20) into (2.19) and make use of an identity for δ functions, we obtain (2.9) directly.

There is one further point to make concerning the consistency of our density-of-states calculation. The

¹⁷ N. Watabe and M. Tanaka, Progr. Theoret. Phys. (Kyoto) 31, 529 (1964).

form factors which we use in evaluating E_k contain the free-electron Fermi momentum k_F . If the density of states which we calculate differs considerably from the free-electron density, the Fermi momentum will, of course, be shifted. To achieve complete internal consistency, we should recalculate the screened form factors using the new k_F , then obtain a new density of states and repeat the process until no further changes occur. We have not gone to these lengths in our calculations.

C. Nonlocal Potentials and the Validity of Perturbation Theory

It should be entirely clear that the expressions we are using to compute the energy and the density of states are well-known results. In the present calculation, we are introducing only two new features which have to do essentially with the nature of the model potential we use in evaluating (2.7). First, we will account for the k dependence of the diagonal matrix element explicitly instead of treating it as a constant or absorbing it into an effective mass. Second, and far more important, we will include the full nonlocality of the form factor in evaluating the second-order contribution to the energy,

$$E_2(k) = -\frac{\Omega_0}{2\pi^2} \int_0^\infty dq q a(q) \int_{-\pi}^\pi d\theta \frac{\sin\theta |w_q(\mathbf{k})|^2}{q + 2k \cos\theta}. \quad (2.21)$$

We have chosen to use the optimum form of the reformulated Heine-Abarenkov model potential^{8,9} in our calculations for two reasons: First, form factors obtained from the reformulated model-potential theory are the only ones available in which the full nonlocality and energy dependence of the potential are accounted for correctly. And second, an extensive program library previously created for other model-potential computations could be readily adapted for use in the density-of-states calculation.

The screened model-potential form factor can be written

$$w_q(\mathbf{k}) = (v_q + v_{dq})/\epsilon(q) + f(\mathbf{k}, \mathbf{q}) + g(q). \quad (2.22)$$

We refer the reader to the paper by Shaw and Harrison⁸ for a detailed discussion of the nomenclature used here. The important point for our present purposes is to note that (2.22) is the sum of several terms which depend only on the magnitude of q and a term, $f(\mathbf{k}, \mathbf{q})$, which depends on both the magnitude and direction of \mathbf{k} and \mathbf{q} . To illustrate the relative importance of the nonlocal term, we have plotted in Figs. 1 and 2 the screened form factors for lithium and indium, evaluated for scattering on the Fermi surface when $q \leq 2k_F$ and for backscattering when $q > 2k_F$. From these form factors we have subtracted the term $f(k_F, q)$ and have plotted the remaining q -dependent terms. It is clear that the nonlocal term represents a substantial contribution to the form factor in both cases. To further emphasize the signifi-

cance of these nonlocal effects, we have plotted in Fig. 3 the form factor for indium as a function of $\cos\theta$ for two different scattering momenta and for the initial state at $k/k_F=0.5$. We have also listed on this figure the values of $w_q(k)$ for backscattering from the $k=0.5k_F$ energy shell and from the Fermi surface. It is clear that variations in the form factor of several hundred percent can occur as k and θ are varied. We now consider precisely why it is crucial not to ignore these variations in evaluating (2.21).

The procedure that Ballentine used in evaluating (2.21) was to replace the nonlocal form factor by a form factor for Fermi-surface scattering. In other words, for $q \leq 2k_F$ the form factor was evaluated only for the case $k=|\mathbf{k}+\mathbf{q}|$, and for $q > 2k_F$ it was evaluated for pure backscattering. This effective local potential, which we will denote by $w_q(k_F)$, depends only on the magnitude of q . The angle integration in (2.21) may then be performed analytically to give

$$\langle E_2(k) \rangle = -\frac{\Omega_0}{4\pi^2 k} \int_0^\infty dq q a(q) w_q^2(k_F) \ln \left| \frac{2k+q}{2k-q} \right|. \quad (2.23)$$

The numerical evaluation of this integral is rather straightforward. However, one immediately notes that the value obtained for $\langle E_2(k) \rangle$ is sensitive to the position of the first form-factor node relative to the initial peak in $a(q)$. This sensitivity is disturbing because we know that $w_q(k_F)$ has a certain degree of arbitrariness inherent in its construction. The position of the first form-factor node has no real physical significance. We know that if a perturbation calculation is carried to all orders, the arbitrariness in the form factor is of no importance whatever. Yet, here we have encountered a second-order perturbation calculation in which the details of $w_q(k_F)$ are critical. We might surmise that perturbation theory is not valid for this calculation.

We find, however, that it is not perturbation theory which is invalid. Rather, it is the crude local approximation made in (2.23) which has led to the difficulty.

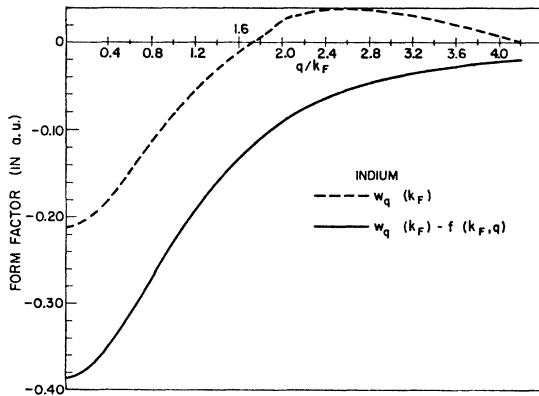


FIG. 2. Optimized model-potential form factor for indium (dashed line) and the \mathbf{k} -independent part of the form factor (solid line).

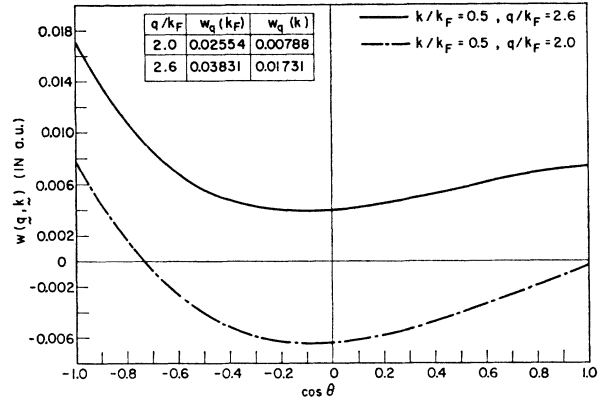


FIG. 3. Form factor for indium as a function of scattering angle for two scattering momenta. The initial state has a wave vector $k=k_F/2$ in both cases. The table gives the corresponding form factors for energy-shell scattering, $w_q(k)$, and Fermi-surface scattering, $w_q(k_F)$, at the same scattering momenta q .

If we use the full nonlocal expression, (2.21), to compute $E_2(k)$, we find that the results are very insensitive to variation of parameters used in constructing the potential. The reason is that, because of the strong angle dependence of the form factors, the effective node sweeps across a wide range as we carry out the integration, and that this range is not strongly dependent on the minute details of the potential. We conclude that reliable calculations of electronic properties of liquid metals, and in particular of the density of states, can be made if the full nonlocal nature of the model potential is included, but that similar calculations using local approximations are likely to be deceptive.

III. EVALUATION OF ELECTRON ENERGY AND DENSITY OF STATES

A. First-Order Corrections

It has been shown by Shaw and Harrison⁸ that the first-order corrections to the electron energy may be determined within a constant (which we set equal to zero) by evaluating the long-wavelength limit of the form factor,

$$E_1(k) = N \langle \mathbf{k} | w | \mathbf{k} \rangle = -\frac{2}{3} E_F + f(k) - f(k_F). \quad (3.1)$$

This correction to the free-electron energy produces a deviation from the free-electron density of states given by

$$\frac{N_1(E)}{N_{FE}(E)} = \left(1 + \frac{1}{k} \frac{\partial f(k)}{\partial k} \right)^{-1}. \quad (3.2)$$

We can regard (3.2) as defining a density-of-states effective-mass ratio, $m^*(k)/m$.^{7,18} It is important to note that this mass is k -dependent.

In Fig. 4, we have plotted $E_1(k)$ as defined by (3.1) for indium and lithium. Though there is a 10% varia-

¹⁸ D. Weaire, Proc. Phys. Soc. (London) **92**, 956 (1967).

TABLE I. Density-of-states effective mass for ten elements evaluated as a function of k/k_F . Comparison is made to Weaire's* results obtained using the original form of the Heine-Abarenkov model potential.

k/k_F	$m^*/m = N_1(E)/N_{FE}(E)$									
	Li	Be	Na	Mg	Al	K	Zn	In	Rb	Cd
0	1.0569	1.0780	0.9619	0.9504	0.9564	0.8707	0.9791	0.9374	0.8294	0.9614
0.1	1.0572	1.0783	0.9620	0.9510	0.9571	0.8712	0.9804	0.9368	0.8300	0.9614
0.2	1.0583	1.0793	0.9624	0.9529	0.9592	0.8728	0.9772	0.9335	0.8313	0.9612
0.3	1.0601	1.0809	0.9630	0.9559	0.9628	0.8754	0.9751	0.9294	0.8338	0.9610
0.4	1.0627	1.0831	0.9639	0.9602	0.9677	0.8792	0.9724	0.9244	0.8373	0.9606
0.5	1.0659	1.0858	0.9651	0.9656	0.9739	0.8842	0.9692	0.9194	0.8420	0.9599
0.6	1.0700	1.0888	0.9666	0.9721	0.9813	0.8904	0.9658	0.9152	0.8480	0.9589
0.7	1.0744	1.0921	0.9684	0.9797	0.9897	0.8980	0.9624	0.9124	0.8554	0.9572
0.8	1.0794	1.0953	0.9705	0.9881	0.9988	0.9071	0.9592	0.9116	0.8645	0.9546
0.9	1.0848	1.0981	0.9730	0.9972	1.0084	0.9176	0.9564	0.9131	0.8755	0.9506
1.0	1.0902	1.1000	0.9758	1.0067	1.0179	0.9295	0.9540	0.9170	0.8884	0.9444
Weaire	1.19	1.28	1.00	1.01	1.04	0.99	0.93	0.89	0.97	0.87

* Reference 18.

tion of $E_1(k)$ over the range of occupied states, there is, clearly, no interesting structure in this variation. We have also evaluated the density-of-states ratio, (3.2) for a group of eight simple metals. The results are given in Table I, and those for lithium and indium are plotted in Fig. 5. Evidently the k variation of the effective mass is not dramatic, so that approximating with a constant effective mass does not introduce any severe errors. The preferable procedure is, of course, to include the k dependence exactly, as we have done. Differences between our results and those obtained by Weaire¹⁸ are due to differences in the potentials used. It is worth noting that the second-order contributions shift the density-of-states effective mass considerably. For this reason, it is worth cautioning against attaching undue significance to the values in Table I, either ours or Weaire's.

B. Second-Order Corrections

We turn now to the second-order corrections to the electron energy. The general expression which we wish to evaluate is given by Eq. (2.21). If we were to treat the form factor as local and include a broadening, we

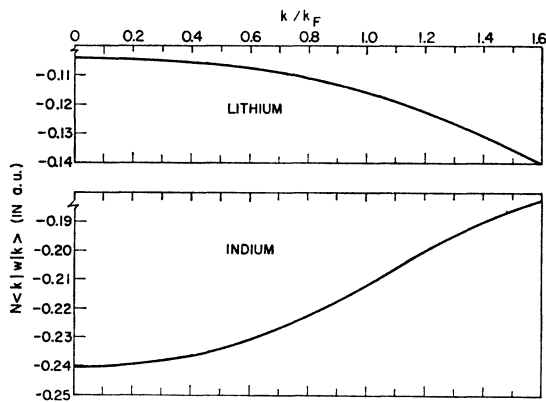


FIG. 4. The first-order corrections to the free-electron energy [Eq. (3.1)] for lithium and indium, as a function of initial-state momentum, k/k_F .

would evaluate

$$\langle E_2(k, \gamma) \rangle = -\frac{\Omega_0}{8\pi^2 k} \int_0^\infty dq q a(q) w_q^2(k_F) \times \ln \left[\frac{(2k+q)^2 + \gamma^2(k)}{(2k-q)^2 + \gamma^2(k)} \right]. \quad (3.3)$$

For computational convenience we have introduced the broadening by replacing k in (2.21) by $k + \frac{1}{2}\gamma(k)$ as suggested by the work of Phariseau and Ziman.¹ This is somewhat different from the procedure used by Ballentine,⁵ but leads to the same effects in the final results. We have varied γ from zero to γ_{\max} , where γ_{\max} is consistent with the mean free path deduced from resistivity measurements.

In order to compare our results with those obtained using a local potential, and to investigate the possible effects due to broadening, we have considered the following four cases:

(1) $E_2(k)$ evaluated using (2.21). This includes all of the important angle and k dependence of the form factors and is of primary interest to us here.

(2) $\langle E_2(k) \rangle$ evaluated with a k -dependent form factor. This is an intermediate approximation which includes various initial states but restricts scattering to energy shells. In this calculation, we have used a lifetime broadening of $\gamma(k) = 0.05k_F$.

(3) $\langle E_2(k) \rangle$ evaluated using (2.23). This case is the perturbation theory equivalent of the approximation used by Ballentine. We should note that for $q > 2k_F$ the form factors which enter are for backscattering. In this calculation, we are making a completely local approximation by ignoring both the k and angle dependence of the form factors.

(4) $\langle E_2(k, \gamma) \rangle$ evaluated using (3.3). We have used completely local form factors in this case and have allowed $\gamma(k)$ to vary from 0 to $0.05k_F$. This case allows us to investigate the importance of lifetime broadening. We have selected the range of γ on the basis of earlier calculations using Ballentine's method.

TABLE II. Summary of the expressions used to compute $E_2(k)$ for each of the cases (1)–(4). Principal-value integrations are implied in cases (1) and (3).

Case	Second-order energy expression
(1)	$E_2(k) = -\frac{\Omega_0}{2\pi^2 k} \int_0^\infty dq q a(q) \int_{-\pi}^\pi d\theta \sin\theta \frac{ w_q(\mathbf{k}) ^2}{q+2k \cos\theta}$
(2)	$\langle E_2(k) \rangle = -\frac{\Omega_0}{8\pi^2 k} \int_0^\infty dq q a(q) w_q^2(k) \ln \left[\frac{(2k+q)^2 + \gamma^2}{(2k-q)^2 + \gamma^2} \right]$ $q < 2k$: energy-shell scattering; $q > 2k$: backscattering $\gamma = 0.05k_F$
(3)	$\langle E_2(k) \rangle = -\frac{\Omega_0}{4\pi^2 k} \int_0^\infty dq q a(q) w_q^2(k_F) \ln \left[\frac{2k+q}{2k-q} \right]$ $q < 2k_F$: Fermi-surface scattering; $q > 2k_F$: backscattering
(4)	$\langle E_2(k, \gamma) \rangle = -\frac{\Omega_0}{8\pi^2 k} \int_0^\infty dq q a(q) w_q^2(k_F) \ln \left[\frac{(2k+q)^2 + \gamma^2}{(2k-q)^2 + \gamma^2} \right]$ $q < 2k_F$: Fermi-surface scattering; $q > 2k_F$: backscattering $0 < \gamma \leq 0.05k_F$

We have summarized in Table II the equations used in each of these calculations.

A program has been written to evaluate $E_2(k)$ for each of these cases. For indium we have used an experimental $a(q)$ due to Ocken and Wagner¹⁹; for lithium we have used the theoretical hard sphere $a(q)$ from Ashcroft and Lekner.¹⁶ The cadmium $a(q)$ was computed by Tomlinson,²⁰ using the Ashcroft-Lekner method. We should remark that the full nonlocal calculation does not appear to be sensitive to minor modifications in $a(q)$. The principal-value integrals were performed numerically using techniques similar to those used previously in the evaluation of screened form factors. The accuracy of these methods has been checked using integrable functions.

The second-order energies are plotted in Figs. 6–8 for lithium, cadmium, and indium. Several important features are immediately evident: In all cases, the exact calculation (case 1) reduces the second-order energy by a factor of 2 compared with the local calculation (case 3). We note, however, that the structure is preserved in the lithium calculation, whereas for cadmium and indium it is considerably reduced. This is a reflection of the fact that form factors for monovalent metals have very weak angular dependence. It is quite obvious from these results that including the k -dependence of form factors but ignoring their angle dependence [case (2)] is a rather bad approximation. We will comment on the reasons for this later. Finally, we note that increasing γ , the lifetime broadening, over a rather large range [case (4)] produces only a slight reduction in structure of the dispersion curves.

The second-order corrections to the density of states can now be determined by differentiating the $E_2(k)$

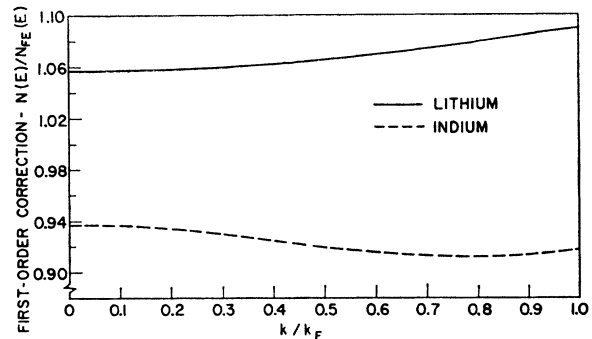


FIG. 5. The first-order corrections to the density of states normalized to the free-electron density for lithium and indium. These curves illustrate the slight k dependence of the density-of-states effective mass.

curves. Since numerical differentiation procedures are notoriously unreliable, we have cross-checked all differentiations graphically. In Fig. 9 we plot the corrections to $N(E)$ for indium arising from $E_2(k)$.

$$\frac{N_2(E)}{N_{FE}(E)} = \left(1 + \frac{\partial E_2(k)}{\partial k} \right)^{-1}, \quad (3.4)$$

for cases (1) and (3). The structure is reduced over 50% by accounting for the nonlocality of the model potential. The structure obtained in case (3) is sensitive to how much the initial peak in $a(q)$ overlaps the form-factor node. If we move the node away from the $a(q)$ peak, the structure can be more than doubled. By

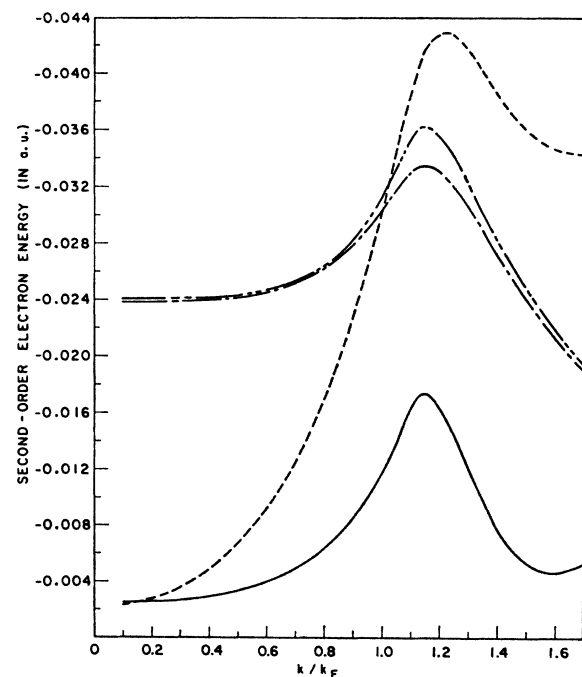


FIG. 6. Second-order corrections to the electron energy for liquid lithium. (Refer to Table II.) The key is as follows: — case (1); --- case (2); - - - case (3); - - - case (4).

¹⁹ H. Ocken and C. H. J. Wagner, Phys. Rev. **149**, 149 (1966).

²⁰ J. L. Tomlinson (private communication).

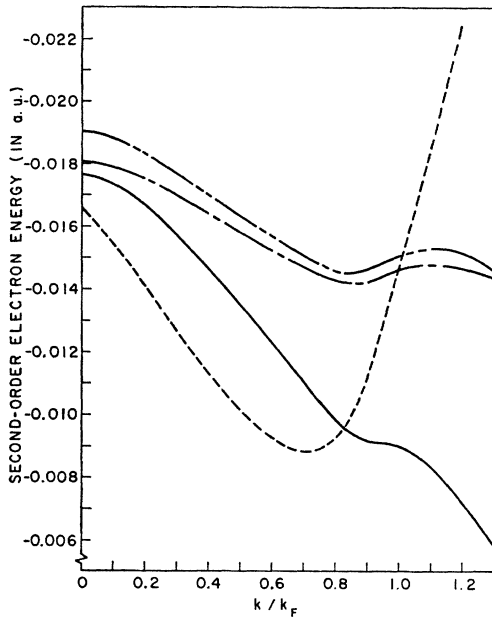


FIG. 7. Second-order corrections to the electron energy for liquid cadmium. The key is the same as in Fig. 6.

contrast, variation in the parameters of the nonlocal form factor produces changes in the density of states which are insignificant. We will discuss the reasons for these results in more detail later. These observations have led us to conclude that the nonlocal calculation gives the more reliable picture of the actual density-of-states structure in a liquid.

To obtain the complete density of states to second order in W , we must use (2.9) and include both first- and second-order terms in the electron energy

$$\frac{N(E)}{N_{FE}(E)} = \left(1 + \frac{1}{k} \frac{\partial f(k)}{\partial k} + \frac{1}{k} \frac{\partial E_2(k)}{\partial k} \right)^{-1}. \quad (3.5)$$

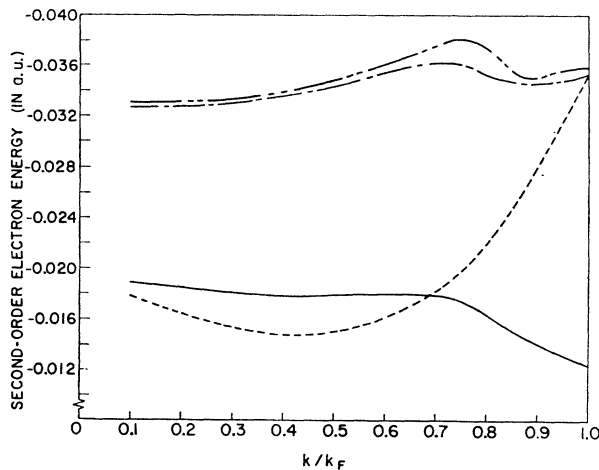


FIG. 8. Second-order corrections to the electron energy for liquid indium. The key is the same as in Fig. 6.

The results of this calculation for lithium, cadmium, and indium are shown in Figs. 10-12. Corresponding results for all four cases are plotted on these figures. We can immediately make two general comments about these results. It is clear that, with the exception of case 2, all methods give very similar density-of-states structure. This is because the structure, but not the magnitude, of $E_2(k)$ is reflected in the density. The nonlocal calculation leads to some smoothing in the density-of-states structure for indium but, essentially, none for lithium. Finally, we observe that the Fermi-surface effective mass for lithium is shifted considerably by the inclusion of second-order corrections; the shift is less pronounced for indium and cadmium.

C. Numerical Interpretation of Results

We can attempt to understand the variations in $E_2(k)$ for the four cases we have considered by studying the behavior of the integrands of the q integration. We will confine our attention here to indium but the situation

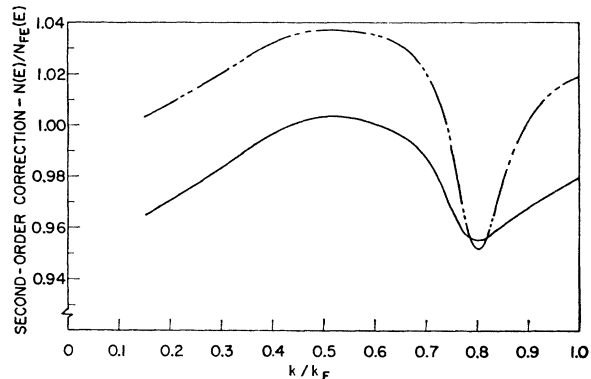


FIG. 9. Second-order corrections to the density of states normalized to the free-electron density [Eq. (3.4)] for liquid indium. Cases (1) (solid line) and (3) (dash-dot-dot) are plotted. The density-of-states structure is reduced by 50% for case (1).

is similar for both lithium and cadmium. We can re-write our expressions for the second-order energy in the form

$$E_2(k) = -\frac{\Omega_0 k_F}{4\pi^2} \int_0^\infty d\eta E(\eta, k), \quad (3.6)$$

$$\eta = q/k_F.$$

In Fig. 13 we have plotted the integrand of (3.6) for cases (1), (2), and (4) at $k/k_F = 0.5$. For case (1) we have indicated the weak logarithmic singularity explicitly. The shoulder at $q = 2k$ for cases (2) and (4) is due to the logarithm. We should remark that $E(\eta, k)$ varies with k , because of the shift in the singularity, and for cases (1) and (2), because of the k dependence of the form factor. However, the general structure for all k is similar to that shown in Fig. 13. The peak in $E(\eta, k)$ at $\eta \cong 1.5$ is a reflection of the corresponding peak in

$a(\eta)$. The size of this peak in cases (2) and (4) is strongly dependent on the position of the form-factor node. However, for case (1), the peak represents an average overlap between the $a(\eta)$ peak and the form-factor node and it is, therefore, not very sensitive to the form-factor parameters. The structure in $E_2(k)$ arises largely from the movement of the logarithmic singularity across this peak as k increases.

The large differences in the magnitude of $E_2(k)$ for the various cases are accounted for by the interesting differences in $E(\eta, k)$ at large values of q . To understand these differences, we refer again to Fig. 3. At large q , the form factor for backscattering from an initial state on the Fermi surface is larger by a factor of 3 than the form factor for backscattering from an initial state at energy $\frac{1}{2}k$. (Recall that we are discussing the case for

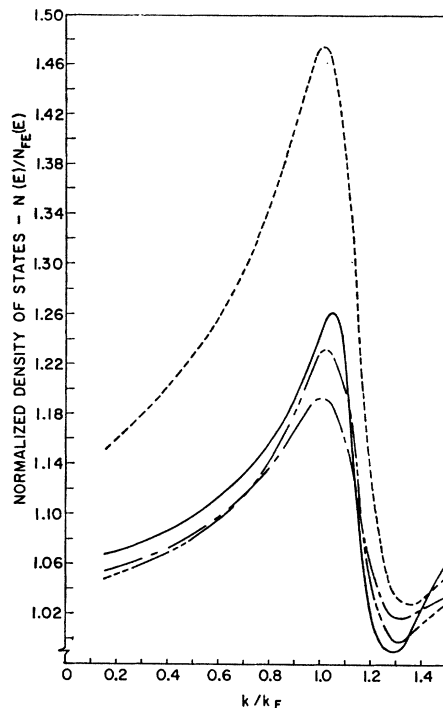


FIG. 10. Normalized density of states as a function of k/k_F for liquid lithium. The key is the same as in Fig. 6.

$k/k_F=0.5$). This difference, when squared, accounts for the order-of-magnitude difference in the second peak for cases (2) and (4). The weighted angle average of the full nonlocal form factor is, following Fig. 3, reduced by another factor of 2 compared to the energy shell scattering case. Hence, the high q peak for case (1) is essentially eliminated.

As k increases over the range of occupied states, the second peak for case (2) changes from a small peak, roughly comparable to that for case (1), to a peak equivalent to the one for Fermi-surface scattering. This accounts for the marked discrepancy of the $E_2(k)$ curve for case (2), as shown in Fig. 8. The second peak in-

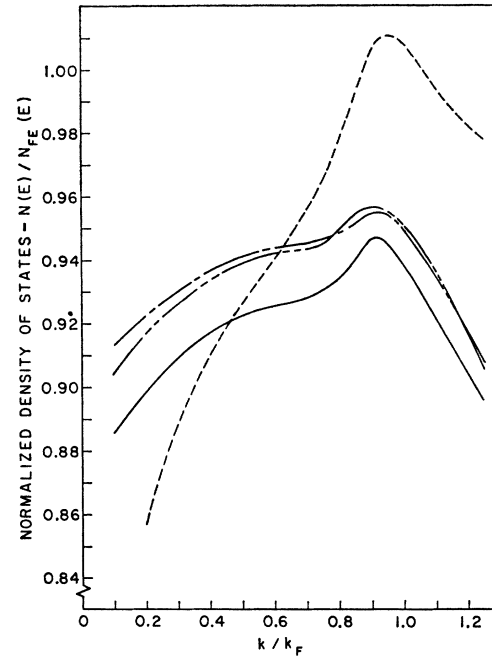


FIG. 11. Normalized density of states as a function of k/k_F for liquid cadmium. The key is the same as in Fig. 6.

creases with increasing k for case (1) as well, but the increase is only by a factor of 2 and does not lead to an appreciable change in $E_2(k)$. It does, however, serve to smooth the dip in $E_2(k)$ near the Fermi surface, and consequently to smooth the density-of-states structure.

We might remark briefly on the situation for lithium. The first peak in $E(\eta, k)$ is very small. This is because the initial $a(\eta)$ peak is above the form-factor node in monovalent lithium. The structure in $E_2(k)$ for lithium is due to the movement of the logarithmic singularity across the second peak. We did not observe comparable structure in indium because the range of k was not extended far enough. The large differences in the magnitude of $E_2(k)$ for the various cases are again due

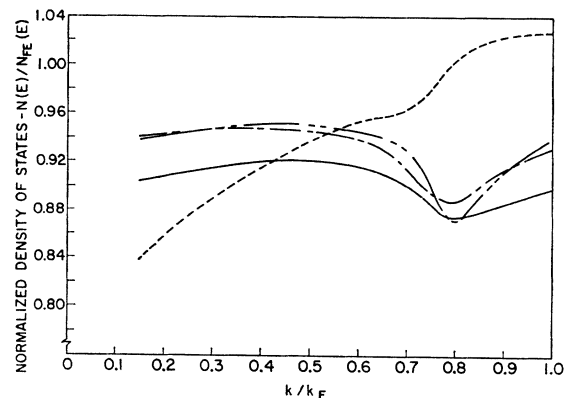


FIG. 12. Normalized density of states as a function of k/k_F for liquid indium. The key is the same as in Fig. 6.

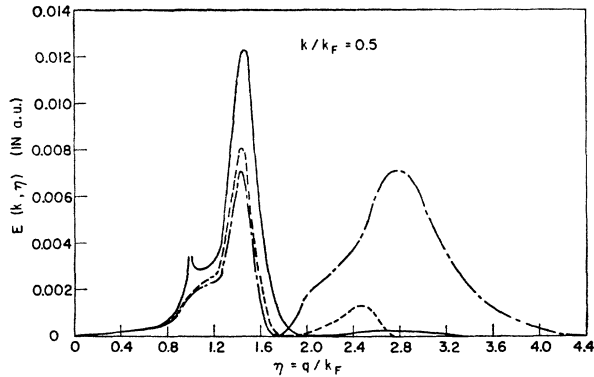


FIG. 13. The integrand of Eq. (3.6) evaluated at $k/k_F=0.5$ for three cases: — case (1); - - - case (2); - · - case (4). Table II gives detailed expressions for $E(\eta, k)$ appropriate to each case. The weak logarithmic singularity for case (1) has been indicated explicitly.

to differences in treatment of scattering from the initial state for large q .

We may summarize our remarks on the second-order dispersion as follows: In each of the cases treated, the structure in $E_2(k)$ is due to the motion of the logarithmic singularity across structure in the integrand, $E(\eta, k)$. The more pronounced the integrand structure, the more pronounced is the final $E_2(k)$ structure. The differences in treating off-energy-shell scattering for the various cases are responsible for the significant differences in the magnitude of $E_2(k)$. We have found that assuming pure backscattering leads to second-order energy corrections which are typically twice as large as those obtained by averaging over all scattering directions.

In calculating second-order corrections to the energy, we have found that the full nonlocal calculation gives substantially different results from the local approximations. The difference is less dramatic for the density of states. Evidently, the structure in both $E_2(k)$ and $N(E)$ is not strongly dependent on the nonlocal effects. We do find some smoothing of structure for indium and cadmium. However, for lithium the density of states is essentially unaltered by the local form-factor approximation. The important point here is that by using a nonlocal potential we obtain a density of states which is insensitive to alterations in the potential. We should emphasize that the apparent similarity of the density of states obtained using the local and nonlocal potentials is largely fortuitous since arbitrary changes in the local potential can produce large changes in the density-of-states structure.

Finally, we should comment on the importance of including lifetime broadening. As expected, the principal effect of lifetime broadening is to smooth structure, both in the dispersion curve and in the density of states. If broadening were introduced into the nonlocal calculation we would evidently observe an even greater smoothing than has already occurred. The essential point is that inclusion of even substantial lifetime

broadening yields only minor changes in the magnitude and structure of second-order corrections to the energy.

IV. DENSITY OF STATES IN A SOLID

It is important to compare the liquid density of states with that in a solid. As we have already remarked, the perturbation expression (2.4) is not valid when \mathbf{k} is near to a boundary of the Brillouin zone. Therefore, to include correctly the distortion of energy surfaces due to zone planes, we must use degenerate perturbation theory. Our aim is to obtain a reasonably precise description of the density of states without resorting to a full band-structure calculation.

The method we have used is to compute the change in volume, $\Omega(E)$, inside a constant energy shell when a single zone plane is introduced. We then superpose the results for all sets of planes which distort the energy shell. We have included only two OPW's in this calculation. That is we diagonalize a two-by-two degenerate matrix and ignore the effects of intersecting planes. It is quite clear⁷ that we do not ignore any significant effects in this scheme. No important density-of-states structure will be overlooked. The nonlocal nature of the model potential introduces far more important effects than those we are ignoring.

Our procedure is, then, to diagonalize the degenerate matrix,

$$\det \begin{vmatrix} \frac{1}{2}k^2 + \langle \mathbf{k} | w | \mathbf{k} \rangle - E & \langle \mathbf{k} | w | \mathbf{k} + \mathbf{q} \rangle \\ \langle \mathbf{k} + \mathbf{q} | w | \mathbf{k} \rangle & \frac{1}{2}(\mathbf{k} + \mathbf{q})^2 + \langle \mathbf{k} + \mathbf{q} | w | \mathbf{k} + \mathbf{q} \rangle - E \end{vmatrix} = 0. \quad (4.1)$$

We have found that the diagonal matrix elements may be accounted for with good accuracy by using the effective-mass approximation. Consequently, we absorb them into the kinetic energy. This has the effect of multiplying all energies by m^*/m .

To compute the volume $\Omega(E)$, it is convenient to define two new variables in terms of the components of \mathbf{k} parallel and perpendicular to the reciprocal-lattice vector, \mathbf{q} ,

$$z = -k_{\parallel} - \frac{1}{2}q, \quad \text{and} \quad \rho = k_{\perp}.$$

The algebraic steps used in computing the volume follow exactly those given by Harrison.⁷ We find that

$$\rho^2 = 2(m^*/m)E - z^2 - \frac{1}{4}q^2 \pm \{z^2q^2 + 4(m^*/m)^2 \times \langle \mathbf{k} | w | \mathbf{k} + \mathbf{q} \rangle \langle \mathbf{k} + \mathbf{q} | w | \mathbf{k} \rangle\}^{1/2}. \quad (4.2)$$

The plus sign is to be used when $z > 0$, the negative sign when $z < 0$. Now the volume inside the surface of energy E is given by

$$\Omega(E) = \pi \int_{z_{(-)}(E)}^{z_{(+)}(E)} \rho^2 dz, \quad (4.3)$$

where the limits, $z_{(\pm)}(E)$, are obtained by setting $\rho = 0$

in (4.2). We find that $z_{(-)}(E)$ is simply

$$z_{(-)}(E) = -\left\{2(m^*/m)E + \frac{1}{4}q^2 + [2q^2(m^*/m)E + 4(m^*/m)^2\langle\mathbf{k}|\mathbf{w}|\mathbf{k}+\mathbf{q}\rangle\langle\mathbf{k}+\mathbf{q}|\mathbf{w}|\mathbf{k}\rangle]^{1/2}\right\}^{1/2}, \quad (4.4)$$

and $z_{(+)}(E)$ is

$$z_{(+)}(E) = \pm\left\{2(m^*/m)E + \frac{1}{4}q^2 - [2q^2(m^*/m)E + 4(m^*/m)^2\langle\mathbf{k}|\mathbf{w}|\mathbf{k}+\mathbf{q}\rangle\langle\mathbf{k}+\mathbf{q}|\mathbf{w}|\mathbf{k}\rangle]^{1/2}\right\}^{1/2}. \quad (4.5)$$

$z_{(+)}(E)$ is negative if the energy surface does not touch the zone plane, zero if it touches but does not extend across the plane, and positive otherwise.

The change in density of states per unit volume due to the one plane in question is obtained from $\Omega(E)$ by

$$\delta N(E, q) = \frac{1}{4\pi^3} \frac{\partial \Omega(E)}{\partial E} - \left(\frac{m^*}{m}\right)^{3/2} N_{FE}(E). \quad (4.6)$$

If we now substitute (4.3) into this equation, recall that $\rho^2(z_{(\pm)})=0$, and use (4.2) to compute $\partial \rho^2/\partial E$, we obtain, simply,

$$\delta N(E, q) = (1/2\pi^2)(m^*/m)[z_{(+)}(E) - z_{(-)}(E)] - (m^*/m)^{3/2} N_{FE}(E). \quad (4.7)$$

To obtain the total density of states we sum $\delta N(E, q)$ over all planes using the appropriate multiplicity, $G(q)$, for each plane

$$N(E) = \sum_q G(q) \delta N(E, q) + \left(\frac{m^*}{m}\right)^{3/2} N_{FE}(E). \quad (4.8)$$

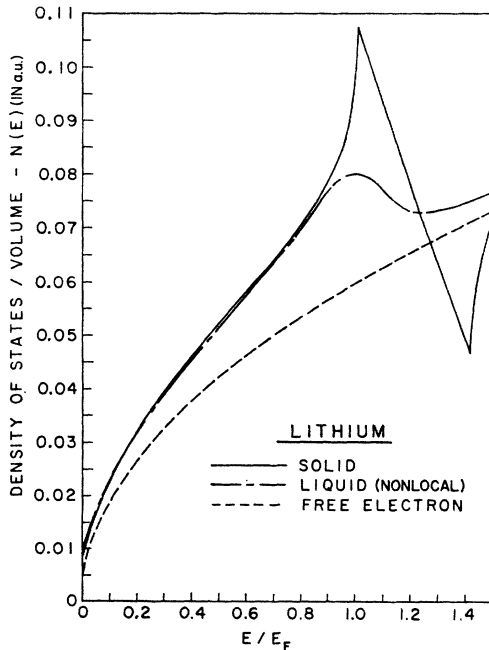


FIG. 14. The density of states for liquid and solid lithium as a function of energy. E_F is the free-electron Fermi energy. The effective mass used in the solid calculation was $m^*/m=1.07$. The liquid curve corresponds to the full nonlocal calculation.

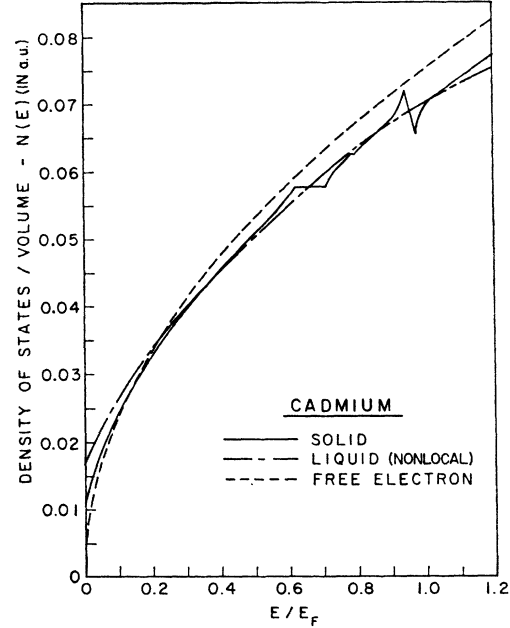


FIG. 15. The density of states for liquid and solid cadmium as a function of energy. E_F is the free-electron Fermi energy. The effective mass used in the solid calculation was $m^*/m=0.96$. The liquid curve corresponds to the full nonlocal calculation.

In arriving at (4.8) we have ignored the E dependence of the form factors, $\langle\mathbf{k}+\mathbf{q}|\mathbf{w}|\mathbf{k}\rangle$, when we evaluated the differential in (4.6). This dependence can be included at the cost of considerable complication in Eq. (4.7). We have found that the change in the density of states due to these terms is less than 1%. Therefore, we have neglected them in the present discussion.

If the actual k dependence of the form factors were included explicitly in (4.1), it would not be possible to obtain simple expression for ρ^2 and z^2 . Yet we know that the form factors vary considerably over the range of occupied states. A simple way to account accurately for the most important part of this variation and still retain the relative simplicity of the expressions we have given is to compute $\langle\mathbf{k}+\mathbf{q}|\mathbf{w}|\mathbf{k}\rangle$ for energy-shell scattering and let

$$k = |\mathbf{k}+\mathbf{q}| = (2E)^{1/2}.$$

In this way, we use in our expressions a matrix element appropriate to the scattering event which actually contributes to the distortion of a given energy shell.

We have evaluated the density of states for lithium, indium, and cadmium using Eq. (4.8). The results are plotted in Figs. 14–16. We have also included the liquid density of states and the free-electron density in each figure for comparison. We should point out that the atomic volumes we have used are the same for both the liquid and solid calculations and are appropriate to the density of the crystalline materials at zero temperature. The density of states of the unperturbed free-electron states is, therefore, the same for the liquid and solid and so are the screening parameters for the potential.

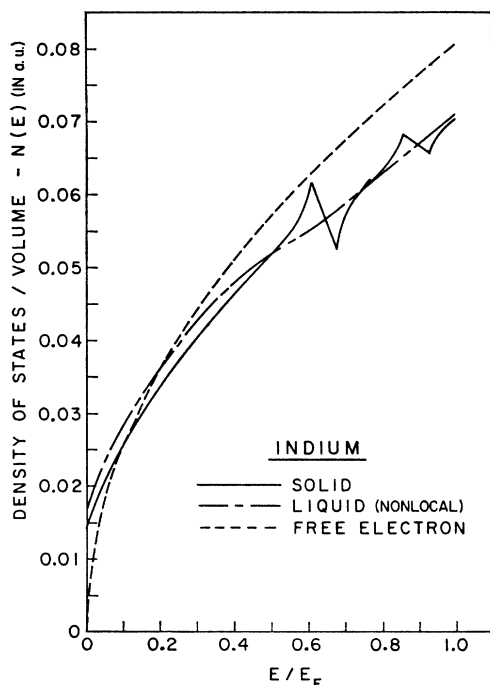


FIG. 16. The density of states for liquid and solid indium as a function of energy. E_F is the free-electron Fermi energy. The effective mass used in the solid calculation was $m^*/m=0.92$. The liquid curve corresponds to the full nonlocal calculation.

Figures 14–16, therefore, illustrate the change in density of states due to change in *structure alone*. In order to obtain the change in the actual density of states, one must remember to scale the curves according to the appropriate free-electron values. Tanaka and Beeby²¹ have argued that a constant-volume approach, such as the one adopted here, is probably more reliable than the alternative constant pressure approach.

In cadmium and indium, the structure in the solid, due to the intersection of constant energy surfaces with zone planes, is rather less pronounced than might be expected. What structure there is becomes considerably smeared out in the liquid. A slight memory of the solid structure can be discerned in the normalized density of states shown in Figs. 11 and 12. However, the curves for the unnormalized density of states in the liquid are very smooth and are remarkably free-electron-like, aside from the effective-mass shifts. For lithium the structure in the solid density of states is more pronounced; and the memory which persists into the liquid is correspondingly more noticeable.

Before comparing our results with experiment we must first locate the true Fermi level. This occurs not at E_F (the free-electron Fermi energy) but is the energy which accommodates 1, 2, and 3 electrons per atom for lithium, cadmium, and indium, respectively. Referring to Figs. 14–16, the Fermi levels were found to occur at

²¹ M. Tanaka and J. L. Beeby, Phys. Rev. Letters **16**, 1088 (1966).

$0.865E_F$ for lithium, $1.01E_F$ for cadmium, and $1.06E_F$ for indium. The effects of this adjustment are most important in the case of lithium. At $E=E_F$ the density of states for solid lithium is 23% higher than for liquid lithium. But at the adjusted Fermi level the difference is only slightly greater than 1%. For solid lithium the ratio of the density of states at the true Fermi level to the free-electron value at $E=E_F$ is 1.27. This is somewhat smaller than the 1.66 obtained by Ham¹⁴ and illustrates the importance of calculating the liquid and solid density of states with the same potential and by the same method.

V. COMPARISON WITH EXPERIMENT

Our calculations on lithium show that the density of states at the adjusted Fermi level decreases by 1.5% on melting. This, however, is the change due to structure alone, since the calculations have been performed for constant atomic volume. The change in volume at the melting point would, by itself, produce a decrease of 1.0% in the free-electron value of the density of states. Combining the structure and volume effects we predict a 2.5% decrease in the density of states of lithium on melting. This is in remarkable agreement with the 2% decrease deduced by Hahn and Enderby²² electron-spin-resonance experiments.

The density-of-states curves for liquid and solid lithium coincide to a striking degree for $E < 0.9E_F$. Since the adjusted Fermi level falls at $0.865E_F$, the profile of filled states is practically identical in the liquid and solid. This goes a long way towards explaining Skinner's observation²³ that the soft x-ray spectrum changes very little on melting. Another interesting feature of the lithium results is that the memory of the zone structure which persists into the liquid state follows quite naturally from the main peak in the liquid-interference function $a(q)$. Consequently, experimental observations of this memory effect, as in the soft x-ray work on aluminum by Catterall and Trotter,²⁴ do not necessarily constitute evidence for local crystallinity in the liquid, as is sometimes claimed.

We find that the density of states at the Fermi level for lithium, cadmium, and indium decreases on melting by 2.5, 0.7, and 0%, respectively. Again, the values for cadmium and indium include the adjustment of the Fermi level and the scaling for the change in atomic volume. It has long been held that the very small changes observed in Knight shift on melting²⁵ provide strong evidence for a correspondingly small change in the Fermi-level density of states. The changes we calculate are indeed very small and, therefore, lend some support to this *general* interpretation of the Knight shift data. Our general conclusion is that the change in

²² C. E. W. Hahn and J. E. Enderby, Proc. Phys. Soc. (London) **92**, 418 (1967).

²³ H. W. B. Skinner, Phil. Trans. Roy. Soc. London **A239**, 95 (1946).

²⁴ J. A. Catterall and J. Trotter, Phil. Mag. **8**, 897 (1963).

the Fermi-level density of states on melting will be appreciable only if the Fermi surface in the solid is in intimate contact with the zone boundaries. This agreement with the Knight shift data is not so encouraging when we come to examine the metals individually. The changes in Knight shift for lithium and indium are essentially negligible^{25,26} and are, therefore, consistent with our calculated densities of states. However, cadmium exhibits a 33% increase in Knight shift^{12,27} whereas our calculated density of states decreases by 0.7%. Ziman's assertion¹³ that the strong change in the Knight shift of cadmium is a density-of-states effect is not borne out by our detailed calculations.

Finally, we consider very briefly the implications of our results with regard to the photoemission experiments on indium.^{10,11} Our prediction for the change in density of states at the solid-liquid transition will be compared with the photoemission data elsewhere.¹¹ Here we will confine our attention to the data on the crystalline solid only. In the nondirect model of the photoemission process, where the optical matrix elements are treated as constant, the energy distribution of photoemitted electrons is essentially a replica of the density of filled states. On the basis of this model, Koyama *et al.*¹⁰ have attributed the pronounced structure observed in the energy distributions to corresponding structure in the density of states, and have presented a theoretical calculation which provides further support for the model. These results are illustrated in Fig. 17. However, their theoretical calculation was performed with an empirical local potential which is probably inadequate for determining the density of states over a wide energy range. A comparison of Figs. 16 and 17 shows that the amplitude of the structure in our solid density of states is about three times smaller and, therefore, insufficient to explain the structure in the energy distribution of

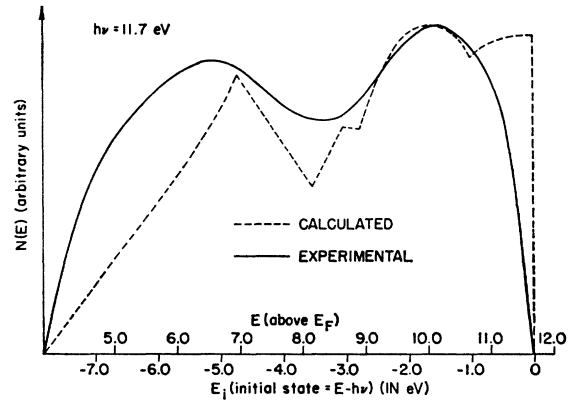


FIG. 17. Comparison of experimental and calculated energy distributions of photoemitted electrons for solid indium, from Koyama, Spicer, Ashcroft, and Lawrence [Phys. Rev. Letters **19**, 1284 (1967)]. Apart from a smooth threshold factor, the theoretical curve is essentially a replica of their calculated density of states.

photoemitted electrons. An alternative explanation for the peak of high-energy electrons observed in photoemission is that it arises through direct transitions between states in the vicinity of the zone boundaries where the *joint* density of states and the optical matrix elements are expected to be rather large. Berglund and Spicer^{28,29} have shown that for the *s* and *p* derived portions of the bands in copper and silver, direct transitions can give rise to important structure in the energy distributions of photoemitted electrons. We hypothesize that a similar situation prevails in indium. This would serve to explain why there is structure in the energy distributions but very little structure in the actual density of states.

ACKNOWLEDGMENTS

We are indebted to Professor W. A. Harrison and Professor W. E. Spicer for their encouragement. Thanks are due also to R. Y. Koyama and E. M. Dickson for stimulating conversations and for showing us their work prior to publication.

²⁵ W. E. Knight, A. G. Berger, and V. Heine, Ann. Phys. (N. Y.) **8**, 173 (1959).

²⁶ J. E. Adams, L. Berry, and R. R. Hewitt, Phys. Rev. **143**, 164 (1966). Note that these authors measured the Knight shift for solid indium at 4°K. F. Rossini (private communication) points out that the constancy of the Knight shift in indium across the melting point has to be inferred by comparison with the results for liquid indium (Ref. 25).

²⁷ E. M. Dickson, thesis, University of California, 1968 (unpublished).

²⁸ C. N. Berglund and W. E. Spicer, Phys. Rev. **136**, A1044 (1964).

²⁹ W. E. Spicer, Phys. Rev. **154**, 385 (1967).